

# THE RESEARCH AND IMPLEMENTATION OF DYNAMIC EPIPOLAR REARRANGEMENT

BingXuan GUO<sup>a</sup>, YuanZheng SHAO<sup>a</sup>, ZhiChao ZHANG<sup>a</sup>, LingYan Dong<sup>a</sup>

<sup>a</sup>State Key Lab of Information Engineering in Surveying Mapping and Remote Sensing,  
Wuhan University, China – mobilemap@gmail.com

Commission WGS-PS, WG IV/9

**KEY WORDS:** Epipolar Image, Dynamic Epipolar Rearrangement , Image Pyramid, Stereoscopic Observation, Memory Pool

## ABSTRACT:

Image re-sampling according to epipolar geometry is a prerequisite for a variety of photogrammetric tasks such as stereoscopic observation. Executing stereoscopic observation by virtue of a pair of epipolar images is a common approach. This paper proposes a new approach to generate epipolar images and measure in stereoscopic environment. In order to improve the accuracy of stereoscopic observation, a dynamic epipolar rearrangement (DER) method is presented. In this method, there is no need to construct the epipolar image pyramid, because the needed epipolar images for measurement is dynamically generated from the original stereo pair pyramid. Then scale the epipolar images and transfer it to the screen buffer directly for stereoscopic observation. The key technology and method for stereoscopic observation, such as constructing pyramid image data structure with high fidelity, dispatching image data by using multi-threaded and memory pool strategy to accelerate the speed of image display, especially the integration operation of integrating the generation of epipolar images with the transfer of the epipolar images to the screen buffer, are deeply investigated.

## 1. INTRODUCTION

At present, digital image acquisition of high resolution, accuracy and multi-spectrum and real-time imagery is coming true, how quickly and efficiently to survey the interested targets and obtain the information from these images has become an active research topic in digital photogrammetry.

The traditional stereoscopic observation strategy is to generate epipolar images after obtaining the stereo pair [1], then the stereopair is tiled and the epipolar images pyramid data structure are constructed from the original stereopair, which create different layers with different resolution [6], [9]. In the course of stereoscopic observation, the images in the epipolar pyramid, which belong to different tiles and layers, are scheduled with the change of the viewpoint.

There are three main truncation errors about the traditional strategy. The first exists in the course of generating epipolar images from the stereopair. The second error is introduced when constructing epipolar images pyramid, which is because the common pyramid algorithm have the loss of accuracy. The third is due to pixel truncation when transfer the epipolar image to screen buffer. The cumulative error caused by the above three errors affect the accuracy that match the cursor with the interested objects in stereoscopic observation, leading to the decrease of measurement accuracy consequently.

To deal with these errors and restrictions, a cylindrical rectification technique was proposed in [2] which used a separate transformation for each epipolar line. However, the technique was complex, omitted many implementation details and worked largely in 3D. A later work, [3] overcame most of these problems, by using the tools of oriented projective geometry to perform a similar nonlinear rectification without using 3D.

In this article, the key technology and method for stereoscopic observation, such as pyramid image, multi-threaded and memory pool strategy, will be researched. In order to improve the accuracy of stereoscopic observation, a dynamic epipolar rearrangement(DER) method is presented. In this method, there is not necessary to construct the epipolar image pyramid, because the needed epipolar images for measurement is dynamically generated from the original stereopair pyramid. Then scale the epipolar images and transfer it to the screen buffer directly for stereoscopic observation.

In Sections 2 the related technologies, such as constructing pyramid image data structure with high fidelity, dispatching image data by using multi-threaded and memory pool, are considered. Section 3 describes the strategy of dynamic epipolar rearrangement. Section 4 presents the systematic integration which illustrates the full process. A proving experiment is also performed in section 5 and the conclusion is drawn in section 6.

## 2. BACKGROUND

### 2.1 Epipolar geometry

The epipolar geometry is the intrinsic projective geometry between two views. It is independent of scene structure, and only depends on the cameras' internal parameters and relative pose [7].

An epipolar line is the intersection of an epipolar plane with the image plane. All epipolar lines intersect at the epipole. An epipolar plane intersects the left and right image planes in epipolar lines, and defines the correspondence between the lines. The epipolar geometry between two views is essentially the geometry of the intersection of the image planes with the pencil

of planes having the baseline as axis (the baseline is the line joining the camera centres). This geometry is usually motivated by considering the search for corresponding points in stereo matching.

There are three degrees of rotational freedom for each camera in total. However, a rotation around the optical axis of a camera will not change the visual data, just the orientation of the image of that camera. Furthermore, in order to keep the cameras in fixation, there will not be any relative tilt between the cameras and a joint tilt around the baseline, will not change the nature of the problem.

## 2.2 Image pyramid

An image pyramid is a series of pixel arrays that represent the same image at successively reduced resolutions. Image pyramids are used extensively in multi-resolution image processing and analysis. In addition, they have also been used in data compression of images and design of computer architecture. The generation of an image pyramid for a given image can be viewed as the application of a series of low-pass filters with successively narrower bandwidths. The input image is fed through this series of filters, and the output of each stage corresponds to the reduced-resolution image at each level of the pyramid. The design of a good pyramid generation process becomes the problem of finding an efficient and effective way to perform such filtering operations. Convolution with limited-size kernels represents fast implementations of low-pass filters. The common approaches for generating pyramid data structure include Gaussian pyramid, Facet pyramid and Wavelet pyramid. In this paper, the Laplacian pyramid is adopted.

## 2.3 Memory pool strategy

There will be some additional costs in the course of using the default memory management function `new/delete` or `malloc/free` in the allocation and release memory stack.

In the receiving system to a certain size memory allocation request, first of all, find the maintenance of internal memory free block list, and some algorithms are needed to find suitable free memory block size. If the free memory block is larger than standard, it is necessary to cut distribution of spare parts and smaller pieces. The system then updates free memory block, completes a memory allocation. Similarly, in the release of memory, the system adds the released memory to the free memory block table. If it is possible, they can block the adjacent idle merged into larger free block.

The default memory management function also takes into account the multi-threaded applications, which increase spending because of the lock for each allocation and release memory. If the applications allocate and release memory frequently in the stack, the performance will be descended. And a large number of fragments of memory are generated, which reduced memory utilization. The default memory allocation and release of natural algorithm also takes into account the performance, but these memory management algorithms are used for meeting more complex, more extensive work. For a specific application, a customized memory pool management algorithm would be offered better performance.

Because the images obtained from the pyramid image database are fixed in size, so a fixed memory pool scheduling algorithms is adopted. Fixed memory pool consists of a range of fixed-size

memory block components, each memory block contain a fixed number and size of the memory cell.

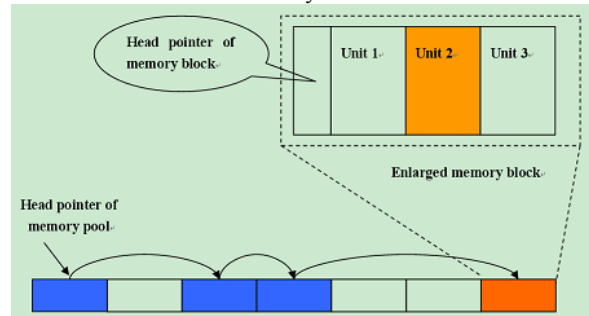


Figure 1. Fixed memory pool

As the figure 1 shows, the total memory pool includes four memory blocks. In the first generation of memory pool, only a memory block is applied, and the pointer is returned as the head pointer to the whole memory pool. With the applications demand more memory, the memory pool is dynamic expand and once again to apply for a new memory blocks, and all memory block are linked together through the pointer.

For an operating system, it has been allocated the same size of four memory blocks to the application. The distribution of speed relatively quickly because of the fixed size. For the application procedures, the pool opened its memory a certain size, but also the internal memory pool of surplus space.

Take the fourth memory block as example, which contains part of block head information of memory pool and three memory modules with same size. Unit 1 and Unit 3 is idle, Unit 2 has been allocated. When the application needs one memory module which allocated from the memory pool, only a simple traversal of all the memory pool block head information, and rapid positioned to the memory block which have free unit. Then according to the block head information, directly positioned to the first vacant unit address and return the address and mark the next free memory modules. When the application releases one memory pool unit, mark this unit vacant in the corresponding block head information.

Compared with the memory management system, the operation of memory pool very quickly, performance optimization in the following main advantages.

- (1) For special circumstances, such as the need for frequent distribution and release of fixed-size memory object, does not require complex distribution algorithms and multi-threaded protection. No additional overhead in maintaining the free memory form.
- (2) Since the opening up a certain amount of memory space for memory pool as a block, thereby to some extent improved procedures localised, and enhance the performance.
- (3) Relatively easy to control the page border alignment and memory byte alignment, which avoid the memory fragment.

## 3. DYNAMIC EPIPOLAR REARRANGEMENT

This paper possess an advantage of generating epipolar images from the original images pyramid dynamically, so in this

section the method of dynamic epipolar rearrangement was introduced.

The generation of horizontal epipolar images is proposed aimed at the situation that the baseline of actual horizontal image is tilted [11]. Based on the simple analysis of the basic epipolar relations, a general formula of non-horizontal epipolar rearrangement in the case of an independent and continuous stereopair relative orientation are presented. The problems exist in the epipolar rearrangement are divided into two main aspects:

- (1) Geodetic coordinate system rotation. Under normal circumstances, the baseline of the stereopair and geodetic coordinate system can not be parallel. If the scan lines of the horizontal images are parallel with the epipolar, the geodetic coordinate system to the baseline direction in the horizontal plane should be rotated.
- (2) Horizontal epipolar rearrangement. Because of the tilt of baseline, the epipolar group and the baseline group generated from the horizontal images are impossible parallel, so the epipolar line rearrangement based on the coplanar conditions should still be implemented.

**3.1 Basic analysis relation**

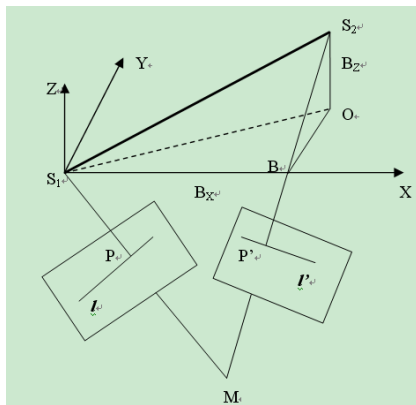


Figure 2. Epipolar line analysis

As shown in figure 3, for the stereopair with fixed baseline  $S_1S_2$ , an epipolar plane is constructed with an arbitrary ground point  $M$  and the baseline. Let the intersecting lines of the epipolar plane and the stereopair are  $l$  and  $l'$ , the project points of  $M$  in left and right image are  $P(x_p, y_p)$  and  $P'$ . Then  $S_1, S_2, P$  and  $P'$  are coplanar, which meets  $\overline{S_1S_2} \cdot (\overline{SP} \times \overline{SP'}) = 0$ . Actually, the arbitrary point  $Q$  in left and right epipolar line (except  $P$ ) are coplanar with the plane constructed with  $S_1, S_2$  and  $P$ .

Take  $S_1$  as the origin of coordinate, let the model coordinate of  $S_2$  is  $(B_x, B_y, B_z)$ , the image space auxiliary coordinate of  $Q$  is  $(X, Y, Z)$ , the image space auxiliary coordinate of  $P$  is  $(X_p, Y_p, Z_p)$ . According to the coplanarity conditions, the points  $S_1, S_2, P$  and  $Q$  meet the following equation:

$$\begin{pmatrix} B_x & B_y & B_z \\ X_p & Y_p & Z_p \\ X & Y & Z \end{pmatrix} = 0 \quad (1)$$

where:

$$\begin{pmatrix} X_p \\ Y_p \\ Z_p \end{pmatrix} = R_L \begin{pmatrix} x_p \\ y_p \\ -f \end{pmatrix} \quad (2)$$

$$\begin{pmatrix} X \\ Y \\ Z \end{pmatrix} = R \begin{pmatrix} x \\ y \\ -f \end{pmatrix} \quad (3)$$

$$R = \begin{pmatrix} a_1 & a_2 & a_3 \\ b_1 & b_2 & b_3 \\ c_1 & c_2 & c_3 \end{pmatrix} \quad (4)$$

where:  $(x, y)$  = the image coordinate of  $Q$ ;  
 $f$  = focal length;  
 $R_L$  = the rotation matrix of left image;  
 $R_R$  = the rotation matrix of right image

$R$  is equal to  $R_L$  when the  $Q$  located in left image. Conversely  $R$  equal to  $R_R$  when the  $Q$  located in right image,

**3.2 Non-horizontal epipolar images generation**

Based on the coplanar conditions, the generations of non-horizontal epipolar images get the corresponding epipolar line directly in the original images, and then rearrange the unparallel epipolar group to parallel epipolar images scan lines.

For the given baseline component, the rotation matrix of stereopair, one point  $P(x_p, y_p)$  in left image and its corresponding image space auxiliary coordinate  $(X_p, Y_p, Z_p)$ , the epipolar line equation can be derived according to Equation 1:

$$y = \frac{A}{B}x + \frac{C}{B}f \quad (5)$$

where:  $f$  = focal length;  
 $x$  = image coordinates;  
 $A = -[m_2a_1 - m_1b_1 + (m_1k_2 - m_2k_1)c_1]$ ;  
 $B = [m_2a_2 - m_1b_2 + (m_1k_2 - m_2k_1)c_2]$ ;  
 $C = [m_2a_3 - m_1b_3 + (m_1k_2 - m_2k_1)c_3]$ ;  
 $m_1 = B_x - B_zk_1$ ;  
 $m_2 = B_y - B_zk_2$ ;  
 $k_1 = X_p/Z_p$ ;  
 $k_2 = Y_p/Z_p$ .

As figure 3 shows, the left end-point of left epipolar lines after rearrangement (Figure 3 (b)) have the same coordinates with the original epipolar lines (Figure 3 (a)). According to the left end-points coordinates of left image, the original left and right epipolar line equations can be deduced by formula 5. Given abscissa  $x$ , its vertical coordinate  $y$  can be determined. By the  $(x, y)$ , the grey level in the rearrangement epipolar lines after performing linear interpolation in  $y$ -axis are calculated.

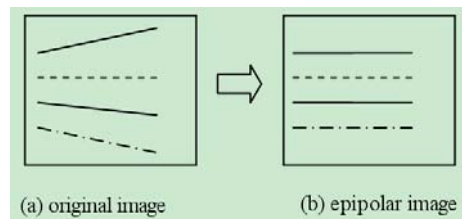


Figure 3. Relation between original and epipolar images

### 3.3 Horizontal epipolar images generation

The essence of the horizontal epipolar line rearrangement is a digital correct process. Under the ideal baseline conditions ( $B_Y = 0, B_Z = 0$ ), the left and right epipolar line, intersected by the epipolar plane and the horizontal images, are parallel and coincide with the scan line. In this condition, the horizontal image coordinates ( $u, v$ ) and the original image coordinates ( $x, y$ ) meet the following relationship:

$$\begin{pmatrix} x \\ y \\ -f \end{pmatrix}_{\text{original}} = \lambda R^T \begin{pmatrix} u \\ v \\ -f \end{pmatrix}_{\text{horizontal}} \quad (6)$$

The projective relationship between two image coordinates is:

$$\begin{cases} x = -f \frac{a_1 u + b_1 v - c_1 f}{a_3 u + b_3 v - c_3 f} \\ y = -f \frac{a_2 u + b_2 v - c_2 f}{a_3 u + b_3 v - c_3 f} \end{cases} \quad (7)$$

However, the actual stereopair baseline is not completely level.  
 ① If the baseline component  $B_Z = 0, B_Y \neq 0$ , then the epipolar lines itself in the horizontal images are completely parallel, but with the angle of scan lines exist. Under this condition, if the x-axis of geodetic coordinate system is rotated to the horizontal component of the baseline direction, the horizontal epipolar images are generated.

② If  $B_Z \neq 0, B_Y \neq 0$ , the epipolar lines itself is not parallel. It is impossible to eliminate the  $B_Z$ , but the geodetic coordinate system can be rotated the angle  $\theta$  to parallel with the baseline, which make the smallest angle between the epipolar lines and the scan lines. Then follow the method of non-horizontal epipolar lines rearrangement, rearrange the epipolar lines of the horizontal images.

The angle  $\theta$  between the epipolar lines and the scan lines can be calculated with the baseline component, that is  $\text{tg}\theta = B_Y/B_X$ . Let  $R_B$  is the rotation matrix which rotates the x-axis of geodetic coordinate system to the horizontal component of the baseline, the rotated baseline component is:

$$\begin{pmatrix} B_{XY} \\ 0 \\ B_Z \end{pmatrix} = R_B \begin{pmatrix} B_X \\ B_Y \\ B_Z \end{pmatrix} \quad (8)$$

where:

$$B_{XY} = \sqrt{B_X^2 + B_Y^2}$$

$$R_B = \begin{pmatrix} B_X / B_{XY} & B_Y / B_{XY} & 0 \\ -B_Y / B_{XY} & B_X / B_{XY} & 0 \\ 0 & 0 & 1 \end{pmatrix}$$

In the horizontal images conditions, based on the Equation (1) and (8), the Equation (9) is deduced:

$$\begin{vmatrix} B_{XY} & 0 & B_Z \\ u_p & v_p & -f \\ u & v & -f \end{vmatrix} = 0 \quad (9)$$

where:

$(u_p, v_p)$  = horizontal image coordinates  
 $(u, v)$  = epipolar image coordinates

So the epipolar line equation of horizontal images is deduced:

$$v = v_p + k(u - u_p) \quad (10)$$

where:

$$k = \frac{B_Z v_p}{B_{XY} + B_Z u_p} \quad (11)$$

According to the above Inferential reasoning formula, the horizontal epipolar images can be generated by the following steps:

(1) Rotate the geodetic coordinates system to the horizontal component direction of baseline, and rotate the rotation matrix of the left and right images, get the horizontal images which parallel with the horizontal component direction of baseline.

(2) Determine the scope of the horizontal images and the epipolar images by the coplanarity equation.

(3) To every line of scan lines in horizontal images:

① According to the points in first row of left images, calculating the epipolar line equation by the formula (10).

② Calculating the longitudinal coordinates ( $v$ ) of epipoalr lines based on the epipolar image abscissa ( $u$ ).

③ Projecting ( $u, v$ ) to the original image, then getting the corresponding coordinates ( $x, y$ ).

④ In the original images, get the gray value of images points ( $u, v$ ) by bilinear interpolation method

### 4. SYSTEM INTEGRATION

By using the dynamic epipolar rearrangement method, the concrete process of stereoscopic observation is as follows:

(1) The first step is to tile the original stereopair, and build the multi-layer image pyramid data structure from low resolution to high resolution. By utilizing the improved pyramid image generation strategy, high fidelity on different image layer can be achieved, and the better measurement result can be gained even using the low resolution image in pyramid. This strategy can resolve the problem on scheduling and displaying the large volume of stereopair.

(2) In the first step, the stereopair pyramid has been built. Then the epipolar images should be generated from the pyramid image. Depending on different viewport, the image in corresponding layer in certain tile is selected from the pyramid image. The selection take advantage of both multi-threading technology and memory pool technology based on page replacement LRU algorithm. So the selected images can be scheduled dynamically. The epipolar lines on the selected images are re-arranged in order to get a pair of epipolar images. According to the difference of the baseline angle, the generation of horizontal or non-horizontal epipolar images is different.

(3) Up to this step, the epipolar images have been produced. Then the epipolar images should be transferred to screen buffer to show. The transfer course will contain truncation error because the epipolar images must be performed scaling transformation before shown in the screen. In order to inhibit this truncation error, integration operation of integrating the generation of epipolar images, as described in step 2, with the scaling operation on epipolar images are executed. After the integration operation, the epipolar images will be scaled and directly transferred to the screen buffer for the stereoscopic observation.

### 5. EXPERIMENTS

An experiment is designed in response to above principles and formulas, which based on the platform VS2005 and OSG (OpenSceneGraph).

The OpenSceneGraph is an OpenSource, cross platform graphics toolkit for the development of high performance graphics applications such as flight simulators, games, virtual reality and scientific visualization.

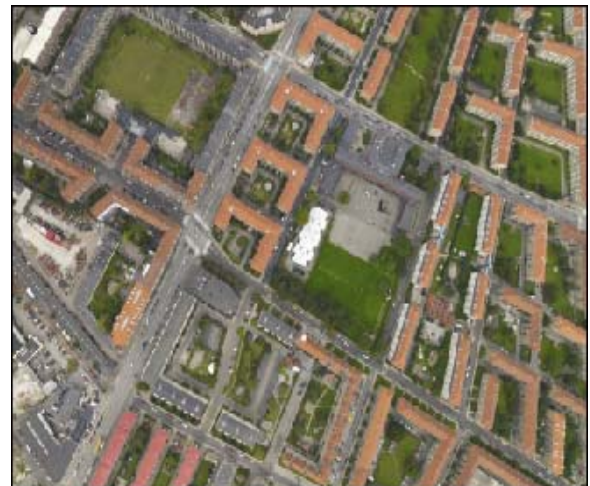
The experiment construct image pyramid from the original image, then carry out the stereoscopic observation based on the application coding with OSG, rearrange the epipolar lines in

accordance with the viewpoint dynamically, measure in the generated epipolar images.

Take the air photograph images as the tested data. The resolution of the image is 6508 \* 4888, the focal length is 34.62mm. An overview of the experimental images is show in Figure 4, including the original stereo pair (a, b) and the generated epipolar images (c, d).



(a) Left original image



(b) Right original image



(c) Left epipolar image



(d) Right epipolar

Figure 4. Experimental images (a, b) and generated epipolar images (c, d)

Calculating the fundamental matrix  $F$ , which is deduced from the ground control points (GCP), is necessary for generating epipolar image. Some corresponding points are selected as the GCP. Three sets of experiments were tested using different numbers of GCP and check points, Table 1. The square root of the estimated variance components and the average absolute values of the resulting  $y$ -parallax are listed in Table 1. The means and standard deviations of the error values in the object space are also listed in the same table.

From Table 1, an insignificant improvement between Experiments 2 and 3 can be seen. Thus, it can be concluded that few GCP can be used for epipolar resampling according to DER. In addition, error standard deviation values of the check points are not significantly different from those of the GCP.

The course of the interior orientation, relative orientation and absolute orientation are completed with the software Virtuoso, which is released by SuperSoft Corp. By checking the generated epipolar images using stereo glasses, no significant disparity from top to bottom. Compare the value of stereoscopic

observation to the GCP, the accuracy and precision are fully meet the production requirements.

Experiment		1	2	3
Num. of GCP		8	24	64
Num. of Check points		128	128	128
$\hat{\sigma}_0\_left$ , pixel		1.4	1.1	0.8
$\hat{\sigma}_0\_right$ , pixel		3.5	3.0	2.7
Mean $ P_Y $ , pixel		1.7	1.5	1.2
GCP (m)	Mean <sub>XY</sub> ±Std <sub>XY</sub>	0±1.315	0±1.126	0±0.734
	Mean <sub>Z</sub> ±Std <sub>Z</sub>	0±4.667	0±4.331	0±3.769
Checkpoints (m)	Mean <sub>XY</sub> ±Std <sub>XY</sub>	0.123±1.286	0.087±1.034	0.066±0.955
	Mean <sub>Z</sub> ±Std <sub>Z</sub>	1.414±5.177	0.916±4.095	0.875±3.822

Table 1. Experimental results of the normalization process

### 6. CONCLUSIONS

This paper proposes a stereoscopic observation system capable of performing dynamic epipolar rearrangement, which is used to obtain geographic information from air photography. Briefly describes the pyramid image generation strategy and methods, memory pool technology is also involved. The concept of epipolar rearrangement and the integration operation of the entire process are investigated deeply. According to the experiment, a conclusion was drawn that adopt the strategy in this paper, a high accuracy and precision of stereoscopic observation can be achieved.

### REFERENCES

[1] Marten Bjorkman, Jan-Olof Eklundh, 2002. Real-time Epipolar Geometry estimation of Binocular Stereo Heads. IEEE Transactions on pattern analysis and machine, 24(3), pp. 425-432.

[2] R. Sebastien, J. Meunier, and J. C. Ingemar, 1997. Cylindrical rectification to minimize epipolar distortion. In Proc. ICVPR, pp. 393-399.

[3] M. Pollefeys, R. Koch, and L. Van, 1999. A simple and efficient rectification method for general motion. In Proc. ICCV, pp. 496-501.

[4] Richard Brooksby, Nicholas Barnes. The memory pool system. Unpublished paper, 2002.

[5] Daniel Oram, 2001. Rectification for any epipolar Geometry [A]. Proceedings of the British Machine Vision Conference [C]. Manchester, UK, pp. 653-662.

[6] Burt, P. Adelson, E., 2003. The Laplacian Pyramid as a Compact Image Code. IEEE, 31(4), pp. 532-540.

[7] Richard Hartley, Andrew Zisserman, 2002. Multiple View Geometry in Computer Vision, Second Edition. Cambridge University Press, pp. 239-241.

[8] Cho, W., T. Schenk, and M. Madani, 1992. Resampling Digital Imagery to Epipolar Geometry, IAPRS International Archives of Photogrammetry and Remote Sensing, 29(B3), pp. 404-408.

[9] Gang Xu and Zhengyou Zhang, 1996. Epipolar geometry in stereo, motion and object recognition. Kluwer Academic Publishers, 1996.

[10] Xiaobo Xu, Hualing Wu, Haiyan Sun, 2006. Algorithm for Epipolarline Images in Digital Photogrammetry. Geospatial Information. Volume 4, Issues 5.

[11] Lihua XU, Ping YAN, Wanshou JIANG. Horizontal Images Based Epipolar Image Generation, 2004. Journal of Zhengzhou University (Engineering Science). Volume 25, Issues 4.

[12] Tao, V. and Y. Hu, 2001. A Comprehensive Study for Rational Function Model for Photogrammetric Processing, Journal of Photogrammetric Engineering & Remote Sensing, 67(12):1347-1357.